Article:
Uddin, SZ, Tanvir, MR and Talukder, MA (2016) A proposal and a theoretical analysis of an enhanced surface plasmon coupled emission structure for single molecule detection. Journal of Applied Physics, 119 (20). 204701. ISSN 0021-8979

https://doi.org/10.1063/1.4952576

A Proposal and a Theoretical Analysis of an Enhanced Surface Plasmon Coupled Emission Structure for Single Molecule Detection

Shiekh Zia Uddin[1], **Mukhlasur Rahman Tanvir**[1], **and**

Muhammad Anisuzzaman Talukder[1,a)]

[1]*Department of Electrical and Electronic Engineering*

Bangladesh University of Engineering and Technology, Dhaka 1205, Bangladesh

[a)]*anis@eee.buet.ac.bd*

Abstract: We propose a structure that can be used for enhanced single molecule detection using surface plasmon coupled emission (SPCE). In the proposed structure, instead of a single metal layer on the glass prism of a typical SPCE structure for fluorescence microscopy, a metal-dielectric-metal structure is used. We theoretically show that the proposed structure significantly decreases the excitation volume of the fluorescently labeled sample, and simultaneously increases the peak SPCE intensity and SPCE power. Therefore, signal-to-noise ratio and sensitivity of an SPCE based fluorescence microscopy system can be significantly increased using the proposed structure, which will be helpful for enhanced single molecule detection, especially, in a less pure biological sample.

1 Introduction

Single molecule detection (SMD) represents the ultimate level of sensitivity of a bio-sensor and has been a long-standing goal. Among SMD techniques, fluorescence based techniques are an obvious choice because of their high sensitivity and ease of detection as a bright signal appears against a dark background [1]. However, SMD using a fluorescence based technique can be difficult for a less pure biological sample due to a poor signal to noise ratio (SNR) [2]. In practice, there will be a background noise signal due to impurities in the sample, emission from optical components, scattered light at the incident wavelength, dark current from the detector, as well as the intrinsic Raman scattering [3]. The background noise signal makes SMD challenging and leave no other choice but to use only a restricted volume of the sample.

Surface plasmon coupled emission (SPCE) based fluorescence microscopy technique can be used for SMD for its capacity to restrict the sample volume that is excited [3]. In this approach, the target molecules, i.e., the sample, are fluorescently labeled and are placed on a thin metal layer, which is deposited on a glass prism [4]. The fluorophore labels are excited by an evanescent light coupled to surface plasmons at the sample-metal layer interface. Surface plasmons at the sample-metal layer interface are excited by an incident light through the prism on to the prism-metal layer interface. Once excited by the evanescent light, fluorophores radiate like dipoles. A part of the radiated light may couple to the metal layer — excite surface plasmons — and emit light from the prism-metal layer interface at a sharply defined angle, which is called SPCE [5–9].

In an SPCE based fluorescence microscopy technique, the excitation volume is inherently limited by the evanescent light coupled to surface plasmons. The part of the radiated light by the fluorophores that couples to SPCE exponentially decreases with distance when the distance of the radiating fluorophores is greater than a critical value [10]. Thus SPCE has inherent capacity

of suppressing the background noise, and therefore, is a promising candidate for SMD [11,12].

However, although in an SPCE based fluorescence microscopy technique, light is emitted only in a sharply defined angle, the intensity of the emitted light is less due to loss in metal [13]. Therefore, detection of a biological sample is difficult when the excitation volume is very limited as in for SMD so that the number of fluorophores that radiate is less. The pursuit of increasing the SPCE light intensity is an active area of research [14–19]. Two approaches are usually used to increase the SPCE light intensity: First, by increasing the radiation of the fluorophores, and second, by increasing the coupling of the radiation of the fluorophores to SPCE. Colloidal metal nano particles suspended in the sample layer or the carbon nano dots at the sample-metal layer interface are found to significantly increase the radiation of the fluorophores so that SPCE intensity and power are increased [20,21]. Fluorophore radiation can also be increased when the fluorophores are trapped in a nanocavity between titanium ceramic nanoparticles and a thin silver layer [22]. By contrast, the coupling of the radiation of the fluorophores to SPCE has been increased by using a grating on the metal layer or by using metal bi-layers of silver and gold [23, 24]. An SPCE based detection system can also be enhanced by increasing the collection efficiency by using external means such as a conical mirror around the hemispherical prism so that SPCE ring is reflected on to a single point [25, 26].

Recently, there have been significant interests in controlling the directional emission of fluorophores by confining fluorophores in a dielectric layer between two thin metal layers [27–29]. Such a structure works as a planar nanocavity and leads to a directional emission of narrow beams normal to the surface. Directional control of the fluorescence emission can also be achieved using a one-dimensional photonic crystal between a metal layer and a dielectric substrate [30]. Such a structure supports optical Tamm plasmon modes and the emission is normal to the surface [31,32].

In this work, we propose a simple planar structure that significantly decreases the excitation volume of the sample, and at the same time, increases both the peak intensity and the coupled power in SPCE so that it can enhance the detectivity of single molecules. In the proposed structure, instead of a single metal layer in a typical SPCE structure, we use a metal-dielectric-metal structure on the glass prism. Considering that the proposed structure is composed of silver-gallium arsenide-silver layers and gallium arsenide (GaAs) is 10 nm thick, we find that the excited sample thickness decreases by $\sim$100 nm, and the peak intensity and the power coupled to SPCE increase by $\sim$2.4 and $\sim$1.4 times, respectively, of that when there is a single silver layer. The SNR of the proposed structure significantly increases as well from that of a typical structure, which is critical for SMD.

The rest of the paper is organized as follows: In Sec. 2, we present the proposed structure. In Sec. 3, we discuss the dispersion relation of the proposed structure. In Sec. 4, we study the detail SPCE dynamics of the proposed structure using full-field finite difference time domain (FDTD) simulations. In Sec. 5, we derive an expression for SNR in SPCE based fluorescence microscopy and use the derived expression to calculate the SNR for the proposed structure. In Sec. 6, we discuss the prospect of SMD using the proposed structure. In Sec. 7, we draw conclusions on the findings.

2 Proposed Structure

In Fig. 1, we show schematic illustrations of a typical structure that supports SPCE and the proposed structure. In Fig. 1(a), in the typical structure for SPCE, a 50 nm silver (Ag) layer is deposited on a hemispherical glass (SiO_2) prism. A 10 nm SiO_2 layer is deposited on the metal layer that acts as a spacer between the Ag layer and the sample layer. The fluorescently labeled sample layer is placed on the spacer layer. In practice, the Ag and spacer layers can be deposited

on a glass slide, which is index-matched to the prism [6, 33]. In Fig. 1(b), in the proposed structure, instead of a single Ag layer, a Ag-GaAs-Ag structure is used. GaAs is optically thick with an index of refraction $\sim$3.5, which is much greater than that of glass. In particular, we use GaAs for its high index of refraction, widespread use in different nanophotonic devices, and ease of deposition as a thin film on a metal layer. However, other dielectric materials that have an index of refraction greater than the substrate and which can be deposited on the metal layers can also be used. We chose the total thickness of the two Ag layers in the proposed structure, i.e., $t_{m1} + t_{m2}$, equal to the thickness of the single Ag layer in the typical structure, i.e., t_m. Typical SPCE structure has a Ag layer of thickness 50 nm [34]. When $t_{m1} = 0$, there is a single metal layer and the dielectric material is above the metal layer acting as a spacer between the fluorophore and metal layer. We keep the thickness of the GaAs layer in between the two Ag layers, t_d, a variable.

In this work, we use a polyvinyl alcohol (PVA) layer of 30 nm as the sample layer. We also use Rhodamine B molecules as fluorophores. Rhodamine B molecules have a peak absorption at a wavelength of 545 nm and a peak emission at 565 nm. In this work, we assume that the fluorophores are excited with a laser source that emits sharp Gaussian pulses at 545 nm and the light is incident from the prism side. The fluorophores in the sample layer subsequently emit light at 565 nm, a part of which is coupled to the Ag layer. The fluorophores are modelled as monochrome electric dipoles oscillating at 565 nm [35]. Since the SPCE dynamics vary with the position of the fluorophores in the sample layer, we keep the positions of the fluorophores fixed so that the performance of the proposed structure can be properly compared with that of a typical SPCE structure.

For SMD, fluorophores have to be excited by a laser source from the prism side, which is often referred to as Kretchmann (KR) configuration [36]. The fluorophores can also be excited

from sample layer side to create SPCE, which is often referred to as reverse Kretchmann (RK) configuration. In KR configuration, if the incidence angle of a p-polarized light on the metal layer matches with a critical angle, θ_{SPR}, surface plasmons are excited and light is evanescently coupled to the sample-metal layer interface. This evanescent light excites the fluorophores in sample layer, which in turn produces SPCE. Since the evanescent light that excites the fluorophores decays exponentially within $\sim$250-300 nm from the interface, fluorophores that are very close to the interface are only excited. Therefore, KR configuration can be used for detecting single molecules attached to the spacer layer on the metal surface in contrast to the RK configuration, which cannot limit the excitation volume [3]. A part of the radiated light by the fluorophores comes out as SPCE in the prism side at an angle θ_{SPCE} such that $\theta_{SPCE} \neq \theta_{SPR}$.

The intensity of SPCE light depends on the intensity of the radiated light by the fluorophores, which in turn depends on the intensity of light that excites the fluorophores. The intensity of SPCE will also depend on the distance of the fluorophores from the metal layer. If the fluorophores are very close to the metal surface, e.g., within $\sim$10 nm, radiation is quenched and the intensity of SPCE decreases significantly [10]. If the distance of the fluorophores increases above $\sim$10 nm, the intensity of SPCE increases to a peak at a critical distance, and then decreases with a relatively slow tail as the distance increases from the critical value.

3 Dispersion Relation of the Proposed Structure

In an SPCE structure, a thin metal layer is bounded by dielectric layers of different refractive indices. The dispersion relation of the typical SPCE structure, as shown in Fig. 1(a), is well studied [37]. The thin metal layer in an asymmetric dielectric environment supports both symmetric and antisymmetric modes [38]. The radiative or leaky symmetric modes are created when a plane wave incident at an appropriate angle from the glass side couples to a surface

plasmon in the metal layer [39]. Only such modes are of interest for the excitation of the fluorophores.

Dispersion relation of a multilayer structure is found by solving Maxwell's equations in each layer and matching them with appropriate boundary conditions. With index inhomogeneity in the z-direction, only p-polarized light with electric field components E_x and E_z, and magnetic field H_y, will excite surface plasmons. If the structure has N number of layers with the j-th layer having dielectric constant ε_j, the dynamics of an incident p-polarized light in the j-th layer can be given by

$$\frac{\partial^2 H_z}{\partial z^2} + (k_j^2 - \beta^2) H_z = 0 \tag{1}$$

and

$$\vec{E} = \frac{i\sqrt{\varepsilon_j}}{\omega c} \vec{\nabla} \times \vec{H}.$$

In each layer, the fields will be a weighted linear combination of the terms $e^{\pm s_j z + i\beta x}$, where $s_j^2 = \beta^2 - k_j^2$ and $k_j = \sqrt{\varepsilon_j} k_0 = \sqrt{\varepsilon_j}\omega/c$.

In an SPCE structure, air and glass layers have fields proportional to $e^{-s_{\text{air}} z}$ and $e^{s_{\text{glass}} z}$, respectively. To make the modes radiative in glass and evanescent in air, s_{glass} and s_{air} have to be imaginary and real, respectively. Therefore, the dispersion curve, i.e., ω vs. β relation, that represents leaky or radiative modes must be in between the light lines for air and glass.

Finding the dispersion relation of the proposed structure is analytically complex due to the presence of a large number of interfaces between layers of different refractive indices. In this work, we calculate the dispersion relations only for the leaky or radiative mode, which is used to excite the fluorophores. We calculate the reflectance $R_p(\omega, \theta)$ of the proposed structure using transfer matrix method [40] for p-polarized plane wave of specific frequency when the incident angle varies in the range $0 \leq \theta \leq \pi/2$. The incidence angle at which the reflectance is

minimum, is the emission angle $\theta_{\mathrm{SPR}}(\omega)$ of the leaky SPR mode. Then the in-plane wavevector can be calculated by

$$\beta(\omega) = \frac{\omega\sqrt{\varepsilon_{\mathrm{glass}}}}{c}\sin\left[\theta_{\mathrm{SPR}}(\omega)\right]. \tag{2}$$

Now, the dispersion relation can be calculated by varying ω.

Figure 2 shows the dispersion relations for a typical SPCE structure and the proposed structure. We note that with the inclusion of the GaAs layer in the proposed structure, the dispersion curve moves further away from the air light line than that of the typical structure. Therefore, the wavenumber s_{air} in the proposed structure increases as $s_{\mathrm{air}}^2 = \beta^2 - \varepsilon_{\mathrm{air}}k_0^2$. The penetration depth in the z-direction in air is $1/s_{\mathrm{air}}$, but the peak electric field in air is proportional to s_{air}. Therefore, the penetration depth of the excitation field in air will decrease but the magnitude of the excitation field will increase in the proposed structure from that in the typical structure.

4 FDTD Simulations

We carry out three-dimensional full-field FDTD simulations to find out the detail SPCE dynamics of the proposed structure. We vary the position of the dielectric layer in between the two metal layers while keeping the total thickness of the two metal layers constant. We also vary the thickness of the dielectric layer. Additionally, we have varied the index of refraction of the dielectric material and found similar results when the index of refraction of the dielectric layer is greater than that of the substrate, and therefore, we do not present those results.

In FDTD simulations, we model Ag, glass, and PVA by their frequency-dependent complex refractive indices as experimentally measured and reported by Palik [41]. We model GaAs and air by constant refractive indices of 3.5 and 1.0 [42]. We assume a three-dimensional computational volume of $20 \times 20 \times 20\ \mu\mathrm{m}^3$ with the SPCE structure at the center. We use a

non-uniform meshing for the computational domain with mesh points separated by less than 4 nm inside and near the metal interface, and by less than 50 nm deep inside prism and air. To simulate an infinite extent in all directions, we use the perfectly matched layer (PML) boundary condition at the boundaries of the computational domain [43]. To calculate the far-field profiles, we project the near-field profiles using their angular spectrum representation.

To study the excitation field, we excite the structures with a Gaussian beam incident at the surface plasmon resonance angle. The appropriate electromagnetic fields are then recorded to determine the penetration depth and the peak excitation field intensity. To study the emission characteristics of fluorophores, excited fluorophores are treated as electric dipoles in our FDTD simulation [44, 45]. The steady-state electromagnetic fields are obtained by calculating the impulse response of the SPCE structure to a dipole source with a Gaussian frequency spectrum centered at 565 nm. FDTD simulation results are validated by matching them with experimental findings and theoretical predictions of Refs. [5, 34].

4.1 Excitation Field

The penetration depth of a typical SPCE structure given in Fig. 1(a) is $\sim$250 nm, i.e., the excitation field decays to $1/e$ of its value at the sample-metal interface at 250 nm away from the interface. The penetration depth of the excitation field in the proposed structure is given in Fig. 3 as the position of the GaAs layer between the two Ag layers changes. We also vary the thickness of the GaAs layer. We note that the penetration depth decreases significantly in the proposed structure. For a fixed GaAs layer thickness, the penetration depth decreases as the GaAs layer is moved from prism to the sample layer, i.e., the thickness of the top Ag layer decreases in the proposed structure. The penetration depth also decreases as the thickness of the GaAs layer increases. In Fig. 4, we show the peak of the excitation field in the sample

layer for the proposed structure for different positions and thicknesses of the GaAs layer. We note that the peak of the excitation field increases when the GaAs layer is moved up, i.e., the thickness of the top metal layer decreases. The peak of the excitation field also increases as the thickness of the GaAs layer increases.

4.2 SPCE

In Figs. 5(a) and 5(b), we show the angle-resolved reflectance characteristics of a typical SPCE structure and the proposed structure with $t_{\mathrm{m1}} = 10$ nm that have been calculated using the transfer matrix method. In both the typical and the proposed structures, the reflectivity is strong for all angles of s-polarized incident light. However, for p-polarized incident light, there is a pronounced dip at the surface plasmon resonance angle, which is also the angle at which SPCE occurs. The proposed structure has the reflectance dip at a greater angle than that of the typical structure, indicating a greater SPCE angle for the proposed structure. In Figs. 5(c) and 5(d), we show the SPCE far-field profiles of a typical and the proposed structures obtained by FDTD simulations. In Figs. 5(e) and 5(f), we show the angle-resolved SPCE for the typical and the proposed structures, respectively. We note the directed emission at the angles predicted by the reflectance minimum.

In Fig. 6, we show the peak SPCE intensity of the proposed structure normalized by that of the typical structure. In Fig. 7, we show the total SPCE power coupled to the prism side of the proposed structure normalized by that of the typical structure. We note that the peak SPCE intensity and the total SPCE power of the proposed structure can be much greater than those of the typical structure. In both cases, we find that the normalized peak intensity and the normalized coupled power reach maximum values when the top metal layer and the dielectric layer have a thickness of 10 nm. The normalized peak intensity and the normalized SPCE

power decrease significantly when t_{m1} is close to zero as the surface plasmons are not excited in the top metal layer.

4.3 Figure of Merit

To enhance the performance of an SPCE based bio-sensor for SMD, the intensity of excitation field of the fluorophores, the peak SPCE intensity, and the SPCE power should be increased. Therefore, a figure of merit (FOM) for an SPCE based bio-sensor can be defined as

$$\text{FOM} = \text{Excitation field intensity} \times \text{Peak SPCE intensity} \times \text{SPCE power.} \tag{3}$$

In Fig. 8, we show the FOM of the proposed structure normalized by that of the typical structure. We note that the FOM is maximum when both the top metal layer and the dielectric layer have a thickness of 10 nm. The increase of the excitation field intensity with $t_{m1} < 10$ nm and $t_d > 10$ nm is offset by the decrease of the peak SPCE intensity and SPCE power.

5 Signal to Noise Ratio

In this section, we will derive an expression for the SNR of an SPCE based bio-sensor with a less pure biological sample. In the detection of a surface activity of a biological sample, the sample layer is not bounded by any interface, rather by the range of the examined chemical activity. The tagged molecules which do not take part in the examined reaction, but are inside the excitation volume, also radiate and contribute to the SPCE light as noise. For reliable detection of the biological sample, the noise SPCE must be suppressed by restricting the excitation volume.

Let us assume that $\mathbf{E}(\mathbf{r}, \mathbf{r}')$ is the electric far-field due to SPCE in the prism side at position

$\mathbf{r} = [x, y, z]$ for a fluorophore located at position $\mathbf{r}' = [x', y', z']$, as shown in Fig. 9. The fluorophore is located at the sample-metal layer interface when $z' = 0$. If the near-field emission of the fluorophore is $\mathbf{E}_{\text{em}}(\mathbf{r}')$ and the response function of the multilayer structure for SPCE is $R(\mathbf{r}, \mathbf{r}')$, then the SPCE at far-field due to a single fluorophore is

$$\mathbf{E}(\mathbf{r}, \mathbf{r}') = R(\mathbf{r}, \mathbf{r}')\mathbf{E}_{\text{em}}(\mathbf{r}'). \tag{4}$$

The near-field radiation $\mathbf{E}_{\text{em}}(\mathbf{r}')$ by a fluorophore will be proportional to the local excitation field $\mathbf{E}_{\text{ex}}(\mathbf{r}')$ and the polarizability f_s of the fluorophore. Since the structure is planar, the response function will exponentially decay as the fluorophore is away from the sample-metal layer interface. Additionally, $\mathbf{E}_{\text{ex}}(\mathbf{r}')$ is an evanescent field, which exponentially decays with distance from the sample-metal layer interface. Therefore, $\mathbf{E}(\mathbf{r}, \mathbf{r}')$ can be written as

$$\mathbf{E}(\mathbf{r}, \mathbf{r}') = f_s e^{-(\alpha_c + \alpha_f)z'} R(\mathbf{r}, [x', y', 0])\mathbf{E}_{\text{ex}}([x', y', 0]), \tag{5}$$

where the parameters α_c and α_f are the exponential decay constants with distance from the sample-metal layer interface for the response function and the excitation field, respectively, $R(\mathbf{r}, [x', y', 0])$ is the response function when the dipole is at $z' = 0$, and $\mathbf{E}_{\text{ex}}([x', y', 0])$ is the excitation field at $z' = 0$. If the fluorophores are distributed with a density $\rho(\mathbf{r}')$ in the sample layer, then the SPCE far-field due to all the fluorophores can be given by

$$\mathbf{E}_{\mathbf{t}}(\mathbf{r}) = \int\int\int dx'dy'dz'\rho(\mathbf{r}')\mathbf{E}(\mathbf{r}, \mathbf{r}'). \tag{6}$$

If the fluorophores are uniformly distributed, i.e., $\rho(\mathbf{r}') = \rho$ and coherently radiating, we can

write

$$\begin{aligned}\mathbf{E_t}(\mathbf{r}) &= f_s\rho\left[\int\int dx'dy'R(\mathbf{r},[x',y',0])\mathbf{E}_{\text{ex}}([x',y',0])\right]\left[\int dz'e^{-(\alpha_c+\alpha_f)z'}\right] \\ &= f_s\rho\left[\int dz'e^{-\alpha z'}\right]\mathbf{E_m}(\mathbf{r}),\end{aligned} \tag{7}$$

where $\alpha = \alpha_c + \alpha_f$ and $\mathbf{E_m}(\mathbf{r}) = \int\int dx'dy'R(\mathbf{r},[x',y',0])\mathbf{E}_{\text{ex}}([x',y',0])$. The parameter $\mathbf{E_m}(\mathbf{r})$ denotes the SPCE electric field created by a monolayer of fluorophores with unit polarizability and located at the sample-metal layer interface.

Similarly, the SPCE magnetic field at position $\mathbf{r}$ due to all the fluorophores in the sample layer is

$$\mathbf{H_t}(\mathbf{r}) = f_s\rho\left[\int dz'e^{-\alpha z'}\right]\mathbf{H_m}(\mathbf{r}), \tag{8}$$

where $\mathbf{H_m}(\mathbf{r})$ denotes the SPCE magnetic field created by a monolayer of fluorophores with unit polarizability and located at the sample-metal layer interface. Now, the radiated power at unit solid angle through an infinitesimal area at position $\mathbf{r}$ is

$$\begin{aligned}P(\mathbf{r}) &= \frac{1}{2}|\mathbf{r}|^2\hat{\mathbf{r}}\cdot\left[\mathbf{E_t}(\mathbf{r})\times\mathbf{H_t^*}(\mathbf{r})\right] \\ &= \frac{1}{2}(f_s\rho|\mathbf{r}|)^2\left[\mathbf{E_m}(\mathbf{r})\times\mathbf{H_m^*}(\mathbf{r})\right]\cdot\hat{\mathbf{r}}\left|\int dz'e^{-\alpha z'}\right|^2 \\ &= (f_s\rho)^2P_m(\mathbf{r})\left|\int dz'e^{-\alpha z'}\right|^2,\end{aligned} \tag{9}$$

where $P_m(\mathbf{r}) = \frac{1}{2}|\mathbf{r}|^2\left[\mathbf{E_m}(\mathbf{r})\times\mathbf{H_m^*}(\mathbf{r})\right]\cdot\hat{\mathbf{r}}$, which is not a function of fluorophore positions $\mathbf{r}'$.

SNR in an SPCE based microscopy for SMD will be the ratio of the SPCE power due to the fluorophores that are tagged to the sample layer to the SPCE power due to the fluorophores that are tagged to molecules outside the sample layer. If we assume that the sample layer has a

thickness of t_s, then

$$\begin{aligned} \text{SNR} &= \left(\frac{f_s\rho_s}{f_n\rho_n}\right)^2 \left|\frac{\int_0^{t_s} dz' e^{-\alpha z'}}{\int_{t_s}^{\infty} dz' e^{-\alpha z'}}\right|^2 \\ &= \left(\frac{f_s\rho_s}{f_n\rho_n}\right)^2 |e^{\alpha t_s} - 1|^2, \end{aligned} \tag{10}$$

where the parameters f_n and ρ_n are the polarizability and the density of the fluorophores outside the sample layer.

We have used the derived expression of SNR in Eq. (9) to calculate the SNR of the proposed structure. In Fig. 10, we show the SNR of the proposed structure normalized by that of a typical structure. The exponential decay constants are calculated from FDTD simulations and the sample layer has a thickness of 30 nm. It is found that the proposed structure significantly increases the SNR by suppressing the background noise.

6 SMD Using the Proposed Structure

For SMD, fluorescence has to be collected from a fluorescently-labeled single molecule. Therefore, in an SMD technique, fluorescence data have to be collected from an extremely small volume, which is small enough to contain a single molecule. However, the size of the volume that has to be excited to detect a single molecule will vary depending on the particular molecule to be detected. Now, the detection volume in an SPCE system will directly depend on the product of two near-field factors: The penetration depth of the excitation field and the distance-dependent coupling of fluorophore radiation to the surface plasmons. The distance-dependent coupling of the radiated power of fluorescence to SPCE varies with the distance of the fluorophore from the metal interface as a skewed bell-shaped relation, with its peak at ~ 25 nm [4, 13]. The full-width at half-maximum (FWHM) of the product of evanescent excitation

field and the distance-dependent coupling for a typical SPCE structure is ~ 50 nm [4,46]. By contrast, for the proposed structure, the FWHM of the product of evanescent excitation field and the distance-dependent coupling is ~ 35 nm. By using techniques as in confocal microscopy, it is possible to limit the lateral dimensions of the detection volume to ~ 200 nm in each direction [4,46].

Since, using the proposed structure, fluorescence can be collected from a much smaller volume than that of a typical SPCE structure, the proposed structure will be a promising candidate for SMD. For example, the proposed structure can be used for SMD for the constituent actin molecules in muscle cells. Using a typical SPCE structure, Borejdo *et al.* showed that two layers of actin monomer filaments with a ~ 30 nm gap between the layers could be detected [4]. In Ref. 4, the fluorophore concentration was ~ 6 fluorescent phalloidin molecules per actin filament. So, a total of ~ 12 actin monomers labeled with phalloidin were detected in the experiment of Ref. 4. Now, with a ~ 35 nm detection thickness in the proposed structure, the number of detected actin monomers will be $\sim 12 \times (35/50) = 8.4$. Additionally, the proposed structure increases the SPCE field by ~ 2.4 times, as shown in Fig. 6. Therefore, the density of fluorescent molecules can be $1/2.4^2 \approx 17.4\%$ smaller than that of a typical structure for same level of detectivity of Ref. 4, so that only $8.4 \times 17.4\% = 1.46$ actin monomers can be successfully detected.

7 Conclusions

We have proposed an enhanced SPCE structure, which can be a promising candidate for SMD. As is required for SMD, the proposed structure significantly decreases the detection volume. Additionally, SPCE intensity of the proposed structure increases so that a significantly smaller density of the sample molecules can be used for the same level of detectivity of that of a

typical structure. Therefore, the smaller detection volume with the smaller density of sample molecules can lead to an application for SMD using the proposed structure. Due to the decrease of the detection volume and the increase of the SPCE intensity, SNR in an SMD technique will increase using the proposed structure.

References

[1] S. Weiss, Science **283**, 1676 (1999).

[2] E. Betzig, and R. J. Chichester, Science **262**, 11422 (1993).

[3] Z. Gryczynski, J. Borejdo, N. Calander, E. Matveeva, and I. Gryczynski, Analytical Biochemistry **356**, 125 (2006).

[4] J. Borejdo, Z. Gryczynski, N. Calander, P. Muthu, and I. Gryczynski, Biophysical Journal **91**, 2626 (2006).

[5] J. R. Lakowicz, Analytical Biochemistry **324**, 153 (2004).

[6] I. Gryczynski, J. Malicka, Z. Gryczynski, and J. R. Lakowicz, Analytical Biochemistry **324**, 170 (2004).

[7] J. R. Lakowicz, Analytical Biochemistry **337**, 171 (2005).

[8] N. Calander, Analytical Chemistry **76**, 2168 (2004).

[9] R. E. Benner, R. Dornhaus, and R. K. Chang, Optics Communications **30**, 145 (1979).

[10] K. Ray, H. Szmacinski, J. Enderlein, and J. R. Lakowicz, Applied Physics Letters **90**, 251 (2007).

[11] C. D. Geddes, I. Gryczynski, J. Malicka, Z. Gryczynski, and J. R. Lakowicz, Journal of Fluorescence **14**, 119 (2004).

[12] J. R. Lakowicz, J. Malicka, I. Gryczynski, and Z. Gryczynski, Biochemical and Biophysical Research Communications **307**, 435 (2003).

[13] J. Enderlein and T. Ruckstuhl, Optics Express **13**, 8855 (2005).

[14] E. Fort and S. Grsillon, Journal of Physics D: Applied Physics **41**, 013 (2008).

[15] P. Mulpur, R. Podila, S. S. Ramamurthy, V. Kamisetti, and A. M. Rao, Physical Chemistry Chemical Physics **17**, 10022 (2015).

[16] A. L. Feng, M. Lin, L. Tian, H. Y. Zhu, H. Guo, S. Singamaneni, Z. Duan, T. J. Lu, and F. Xu, RSC Advances **5**, 76825 (2015).

[17] S. Venkatesh, P. K. Badiya, and S. S. Ramamurthy, Physical Chemistry Chemical Physics **18**, 681 (2016).

[18] P. Mulpur, R. Podila, K. Lingam, S. K. Vemula, S. S. Ramamurthy, V. Kamisetti, and A. M. Rao, The Journal of Physical Chemistry C **117**, 17205 (2013).

[19] S. H. Cao, T. T. Xie, W. P. Cai, Q. Liu, and Y.-Q. Li, Journal of the American Chemical Society **133**, 1787 (2011).

[20] M. H. Chowdhury, K. Ray, C. D. Geddes, and J. R. Lakowicz, Chemical Physics Letters **452**, 162 (2008).

[21] S. Venkatesh, P. K. Badiya, and S. S. Ramamurthy, Chemical Communications **51**, 7809 (2015).

[22] V. Srinivasan and S. S. Ramamurthy, The Journal of Physical Chemistry C **120**, 2908 (2016).

[23] J. S. Yuk, B. D. MacCraith, and C. McDonagh, Biosensors and Bioelectronics **26**, 3213 (2011).

[24] J. S. Yuk, E. F. Guignon, and M. A. Lynes, Chemical Physics Letters **591**, 5 (2014).

[25] D. S. Smith, Y. Kostov, and G. Rao, Applied Optics **47**, 5229 (2008).

[26] B. Ge, Y. Ma, C. Kuang, D. Zhang, K. C. Toussaint, S. You, and X. Liu, Optics Express **23**, 13159 (2015).

[27] S. Dutta Choudhury, R. Badugu, K. Nowaczyk, K. Ray, and J. R. Lakowicz, The Journal of Physical Chemistry Letters **4**, 227 (2012).

[28] S. Dutta Choudhury, R. Badugu, K. Ray, and J. R. Lakowicz, The Journal of Physical Chemistry C **117**, 15798 (2013).

[29] S. Dutta Choudhury, R. Badugu, K. Ray, and J. R. Lakowicz, The Journal of Physical Chemistry C **119**, 3302 (2015).

[30] R. Badugu, E. Descrovi, and J. R. Lakowicz, Analytical biochemistry **445**, 1 (2014).

[31] Y. Chen, D. Zhang, L. Zhu, R. Wang, P. Wang, H. Ming, R. Badugu, and J. R. Lakowicz, Optica **1**, 407 (2014).

[32] Y. Chen, D. Zhang, D. Qiu, L. Zhu, S. Yu, P. Yao, P. Wang, H. Ming, R. Badugu, and J. R. Lakowicz, Laser & Photonics Reviews **8**, 933 (2014).

[33] K. Toma, M. Vala, P. Adam, J. Homola, W. Knoll, and J. Dostlek, Optics Express **21**, 10121 (2013).

[34] I. Gryczynski, J. Malicka, K. Nowaczyk, Z. Gryczynski, and J. R. Lakowicz, The Journal of Physical Chemistry B **108**, 12073 (2004).

[35] N. Calander, The Journal of Physical Chemistry B **109**, 13957 (2005).

[36] S. A. Maier, *Plasmonics: fundamentals and applications* (Springer Science & Business Me- dia, 2007).

[37] E. Economou, Physical Review **182**, 539 (1969).

[38] H. Raether, *Surface plasmons on smooth surfaces* (Springer, 1988).

[39] J. Pitarke, V. Silkin, E. Chulkov, and P. Echenique, Reports on Progress in Physics **70**, 1 (2006).

[40] S. J. Orfanidis, *Electromagnetic waves and antennas* (Rutgers University New Brunswick, NJ, 2002).

[41] E. D. Palik, *Handbook of optical constants of solids* (Academic Press, 1998).

[42] D. E. Aspnes, S. Kelso, R. Logan, and R. Bhat, Journal of Applied Physics **60**, 754 (1986).

[43] J. P. Berenger, Journal of Computational Physics **114**, 185 (1994).

[44] L. Novotny and B. Hecht, *Principles of nano-optics* (Cambridge University Press, 2012).

[45] J. R. Lakowicz, *Principles of fluorescence spectroscopy* (Springer Science & Business Media, 2007).

[46] Z. Gryczynski, I. Gryczynski, E. Matveeva, N. Calander, R. Grygorczyk, I. Akopova, S. Bharill, P. Muthu, S. Klidgar, and J. Borejdo, in *Biomedical Optics (BiOS) 2007*, (International Society for Optics and Photonics, 2007), pp. 64440G.

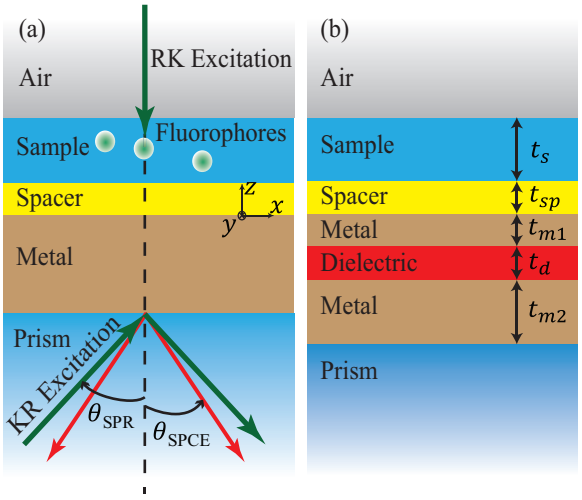

Fig. 1: Schematic illustrations of (a) Typical structure used for SPCE based fluoroscence microscopy with different excitation schemes for the fluorophores and (b) Proposed structure for SPCE based fluoroscence microscopy.

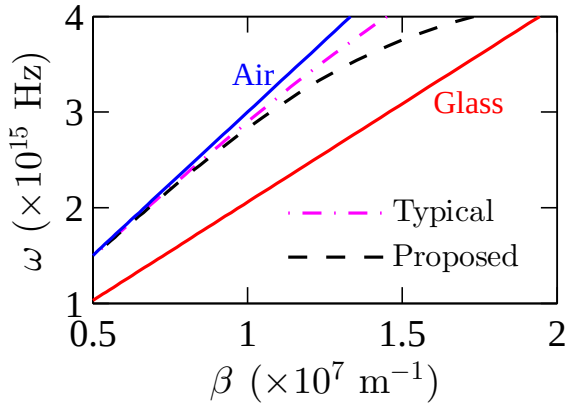

Fig. 2: Dispersion relation of a typical SPCE structure and the proposed structure. In the proposed structure, we assume $t_{m1} = 10$ nm and $t_d = 10$ nm. The most left and right straight lines are the light lines for air and glass, respectively.

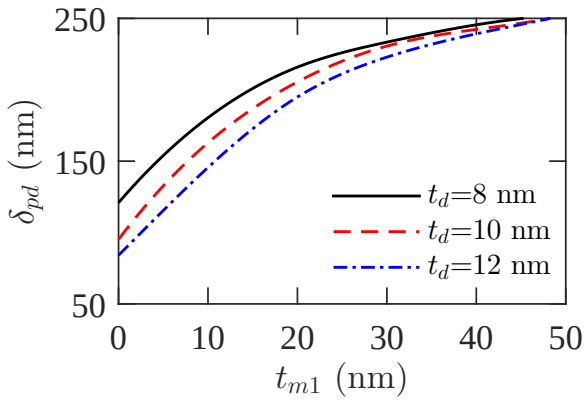

Fig. 3: Penetration depth (δ_{pd}) of the excitation field for fluorophores of the proposed structure against thickness of the top metal layer (t_{m1}) for different GaAs layer thicknesses (t_{d}).

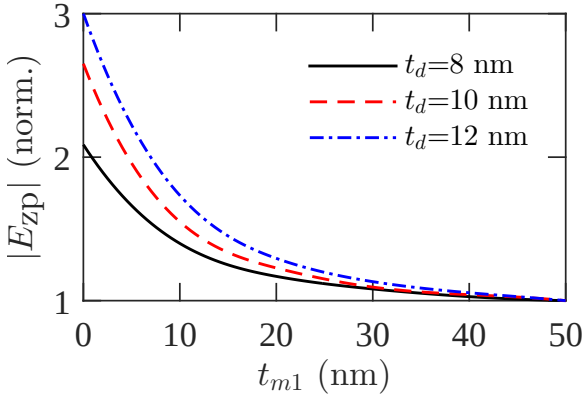

Fig. 4: Peak excitation field $|E_{zp}|$ of the proposed structure normalized by that of the typical structure $|E_{zpc}|$ against top metal layer thickness (t_{m1}) for different GaAs layer thicknesses (t_{d}).

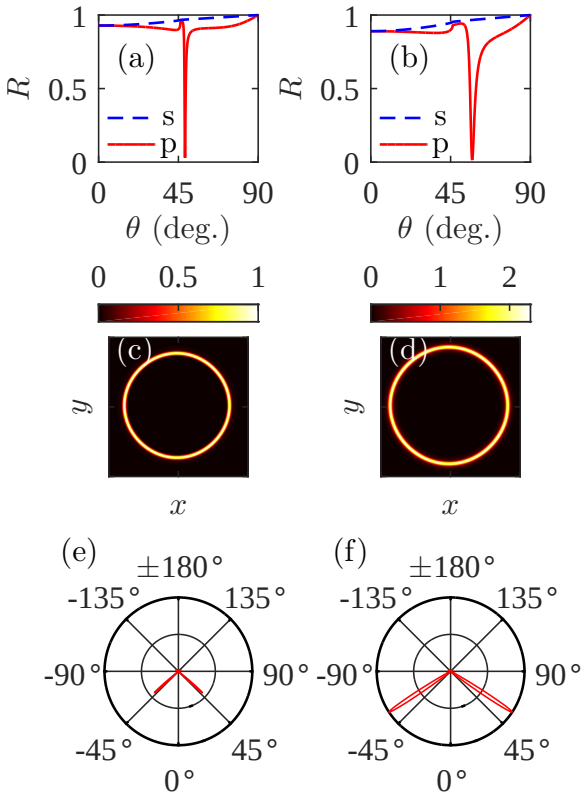

Fig. 5: Reflectance (R) characteristics against incident angle for p- and s-polarized light of (a) a typical SPCE structure and (b) the proposed SPCE structure, Far-field profile of SPCE electric field of (c) a typical structure and (d) the proposed structure in the x-y plane. Angle resolved SPCE intensity of (e) a typical structure and (f) the proposed structure. In each case, we assume $t_{\mathrm{m1}} = 10$ nm and the incident light has a wavelength of 565 nm.

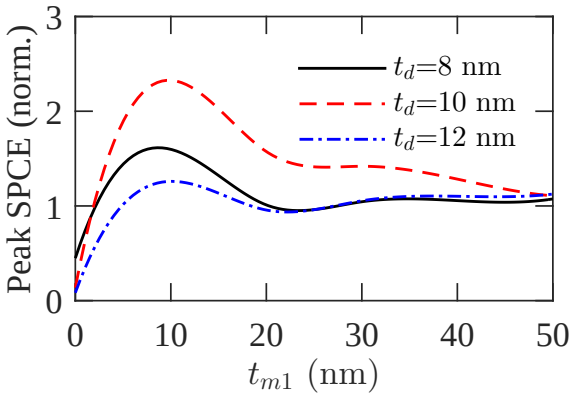

Fig. 6: SPCE peak intensity of the proposed structure normalized by that of the typical structure against top metal layer thickness (t_{m1}) for different GaAs layer thicknesses (t_{d}).

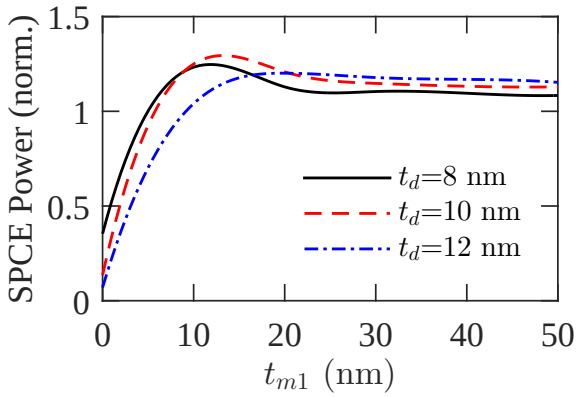

Fig. 7: SPCE power of the proposed structure normalized by that of the typical structure against top metal layer thickness (t_{m1}) for different GaAs layer thicknesses (t_d).

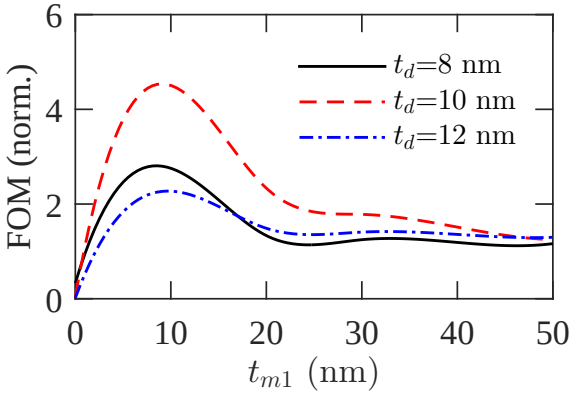

Fig. 8: Figure of merit (FOM) of the proposed structure normalized by that of the typical structure against top metal layer thickness (t_{m1}) for different GaAs layer thicknesses (t_d).

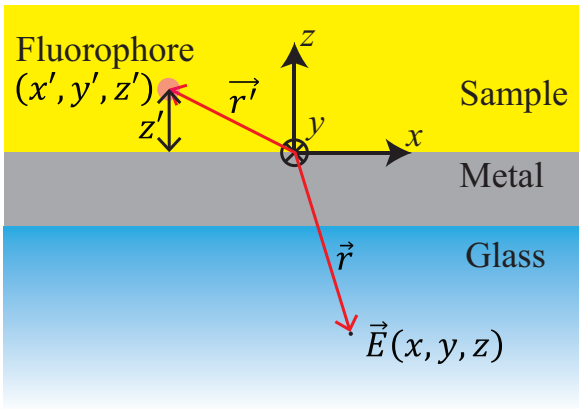

Fig. 9: Schematic illustration of an SPCE structure showing the positions of a fluorophore and measurement of SPCE field in glass prism.

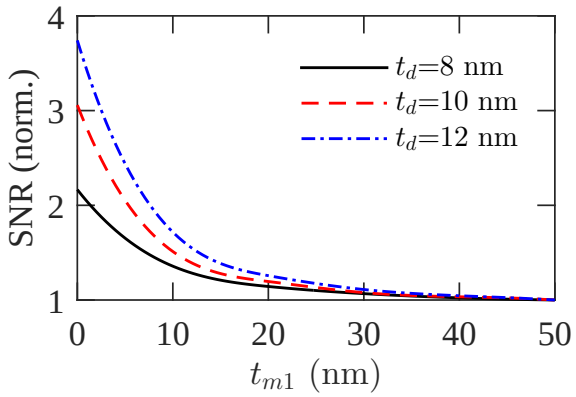

Fig. 10: SNR of the proposed structure normalized by that of the typical structure against top metal layer thickness (t_{m1}) for different GaAs layer thicknesses (t_{d}).